Journal of the Australian Ceramic Society (2018) 54:401–410
https://doi.org/10.1007/s41779-017-0166-z

RESEARCH

Hard and tough Al_2O_3-SiC-CNT hybrid ceramic nanocomposite produced by molecular level mixing and spark plasma sintering

N. Saheb [1,2] · K. Mohammad [1]

Received: 15 April 2017 / Revised: 9 September 2017 / Accepted: 28 November 2017 / Published online: 4 December 2017

Abstract

This work reports a simultaneous improvement in both the hardness and toughness of an alumina Al_2O_3-SiC-CNTs hybrid ceramic nanocomposite. The nanocomposite powder was synthesized using sonication and molecular level mixing (MLM) and was sintered at 1500, 1550, and 1600 °C for 10 min by the spark plasma sintering (SPS) method. The influence of sintering temperature on the microstructure and properties was investigated. The dispersion of silicon carbide (SiC) nanoparticles and carbon nanotubes (CNT) in the powder and consolidated samples was characterized using a field emission scanning electron microscope equipped with energy dispersive spectroscopy. The microhardness and fracture toughness of the samples were measured using a hardness tester. The synthesized nanopowder and the consolidated samples revealed a uniform distribution of the SiC and CNT reinforcements. The relative density of the sintered samples increased from 90.36 to 98.91% as a result of an increase in sintering temperature from 1500 to 1600 °C. The Al_2O_3-5SiC-1CNTs sample, which was sintered at 1600 °C for 10 min, possessed the highest hardness and fracture toughness values of 23.32 GPa and 7.10 MPa.$m^{1/2}$, respectively. This finding constitutes an increase in the hardness and fracture toughness of 25.65 and 96.67%, respectively, compared to monolithic alumina sintered at 1500 °C for 10 min.

Keywords Molecular level mixing · Spark plasma sintering · Alumina hybrid nanocomposites · Densification · Hardness · Fracture toughness

Introduction

The high stiffness and hardness of monolithic ceramic materials makes them attractive for various applications [1]. However, the intrinsic brittleness and limited fracture toughness of these materials restricts their use in many structural applications. Fortunately, the development of composites [2], nanocomposites [3], and hybrid nanocomposites [4–7] has helped to remove these limitations. The reinforcement of ceramics using two nanoscale phases that have different morphologies and/or attributes, the so-called hybrid microstructure design, is a new methodology that has been adopted to develop nanocomposites with tailored nanostructures and improved mechanical properties. However, there are challenges in developing ceramic nanocomposites that are both high-performance and cost-effective for commercial applications. Achieving a uniform distribution or dispersion of nanoscale reinforcements in the matrix is a major problem to be overcome in order to synthesize homogenous nanocomposite powders. Additionally, for powder metallurgy processes, creating the desired high density using conventional sintering methods requires the use of relatively high sintering temperatures and long sintering times. This usually results in grain growth and a loss of nanostructured features. However, promising new synthesis and sintering methods such as molecular-level mixing [4] and spark plasma sintering [5] have enabled researchers to develop homogenous and almost fully dense ceramic hybrid nanocomposites.

Molecular-level mixing (MLM) is a novel fabrication process developed to synthesize carbon nanotube (CNT) reinforced metal matrix nanocomposites [8]. The advantages of MLM include the homogenous distribution of the reinforcing agent and the high interfacial strength due to chemical

✉ N. Saheb
nouari@kfupm.edu.sa

[1] Department of Mechanical Engineering, King Fahd University of Petroleum and Minerals, Dhahran 31261, Saudi Arabia

[2] Centre of Research Excellence in Nanotechnology, King Fahd University of Petroleum and Minerals, Dhahran 31261, Saudi Arabia

bonding between the reinforcing agent and the matrix. Moreover, the reinforcement material is mainly located within the matrix powder rather than on the surface of the powder. The MLM method has been demonstrated to successfully synthesize homogenous alumina nanocomposites reinforced by reduced graphene oxide [9] and by CNTs [10]. More recently, the MLM technique was extended to the uniform dispersion of CNTs and SiC nanoparticles in an Al_2O_3 matrix [4]. Spark plasma sintering [11] is a novel consolidation method in which a uniaxial pressure and a pulsed direct electrical current are simultaneously applied. SPS is used to consolidate powdered materials and to obtain fully dense materials with controlled microstructures and properties. The advantages of SPS include the following: (i) extremely high heating rates, (ii) enhanced densification, even at relatively low temperatures for short times, (iii) limited grain growth, and (iv) promotion of diffusion mechanisms. This enables the retention of the excellent intrinsic properties of nanopowders in the final bulk composite material [12, 13]. Furthermore, the process is binder-less, direct, and cost-effective compared to other powder metallurgy processes.

Aluminum oxide, or alumina [14], is a ceramic material widely used to manufacture cutting tool inserts [15] and dental implants for machining and biomedical applications, respectively. Moreover, alumina is a material of choice for chemical and electrical insulators [16] and for use in armories [17]. However, its use in many structural applications is restricted by its low fracture toughness. The addition of a single nanoreinforcement to alumina was reported to improve its mechanical properties [3]. Additionally, reinforcing alumina with hybrid nanoscale reinforcements such as silicon carbide nanoparticles [18] or CNTs [19] that have various morphologies and attributes has led to further improvements in mechanical properties [4, 5, 7, 20, 21]. In previously published work [4], the authors have developed a novel procedure via molecular level mixing to synthesize an Al_2O_3-SiC-CNT hybrid nanocomposite powder. The composite was sintered at 1500 °C for 10 min and demonstrated improved fracture toughness (by approximately 33%) and slightly reduced hardness (by approximately 4%) with respect to monolithic Al_2O_3 sintered at similar conditions. The moderate improvement in fracture toughness and the slight decrease in hardness were attributed to the low density of the final composite. The objective of this work is to explore the possibility of developing a fully dense, hard, and tough Al_2O_3-SiC-CNT hybrid nanocomposite.

Materials and methods

Aluminum nitrate nonahydrate ($Al(NO_3)_3{\cdot}9H_2O$) was used as a precursor to form alumina. MWCNTs were produced by chemical vapor deposition. SiC_β (97.5% purity and particle size between 45 and 55 nm) was obtained from nanostructured and amorphous material. In addition, α-Al_2O_3 (99.85% purity and average particle size of 150 nm, supplied by ChemPUR, Germany) was sintered and used as a reference sample. The detailed procedure to synthesize the Al_2O_3-5SiC-1CNTs nanocomposite powder with a uniform distribution of SiC nanoparticles and CNTs via sonication and molecular level mixing was reported in a recent study [4]. A summary of the procedure is provided in this work. The CNTs were functionalized to generate negatively charged functional groups on their surfaces, and metallic ions were obtained through the dissociation of a metallic salt in an organic solvent. Next, bonding occurs between the functionalized CNTs and the metallic ions in the prepared slurry. The SiC nanoparticles were dispersed in the slurry using high-energy probe sonication. This was followed by drying and firing the mixture to form an amorphous Al_2O_3 matrix embedded with CNTs, which crystallized during sintering. The Al_2O_3-5SiC-1CNTs nanocomposite powder was prepared using a sonication time of 2 h and then sintered at 1500 °C for 10 min, with a heating rate of 100 K/min and a compaction pressure of 50 MPa. The sample showed a uniform distribution of the reinforcing agents and had a similar relative density, hardness, and fracture toughness compared to the sample prepared using a sonication time of 24 h and sintered under the same conditions [4]. Therefore, a sonication time of 2 h was selected to lower the overall cost and to avoid degradation of the CNTs. The sintering temperature was increased to 1550 and 1600 °C to improve the densification. The compaction pressure, heating rate, and holding time were kept constant at 50 MPa, 100 K/min, and 10 min, respectively. The monolithic alumina nanopowder was sintered under similar conditions, but the temperature was fixed at 1500 °C because at this temperature full densification occurred. The powders were consolidated using fully automated spark plasma sintering equipment (FCT system, Model HDP 5, Germany). The microstructure of the prepared material was characterized as needed, using field emission scanning electron microscopy (FE-SEM), X-ray mapping, and X-ray diffraction. A density determination kit and a hardness tester were used to evaluate the density and the mechanical properties of the developed materials, respectively. More details on the characterization of the composite's microstructure and the determination of mechanical properties can be found elsewhere [4].

Results and discussion

Microstructure

The transmission electron microscopy images of the SiC, CNT, and Al_2O_3 nanopowders are presented in Fig. 1. The SiC nanopowder appears to have a wide particle size

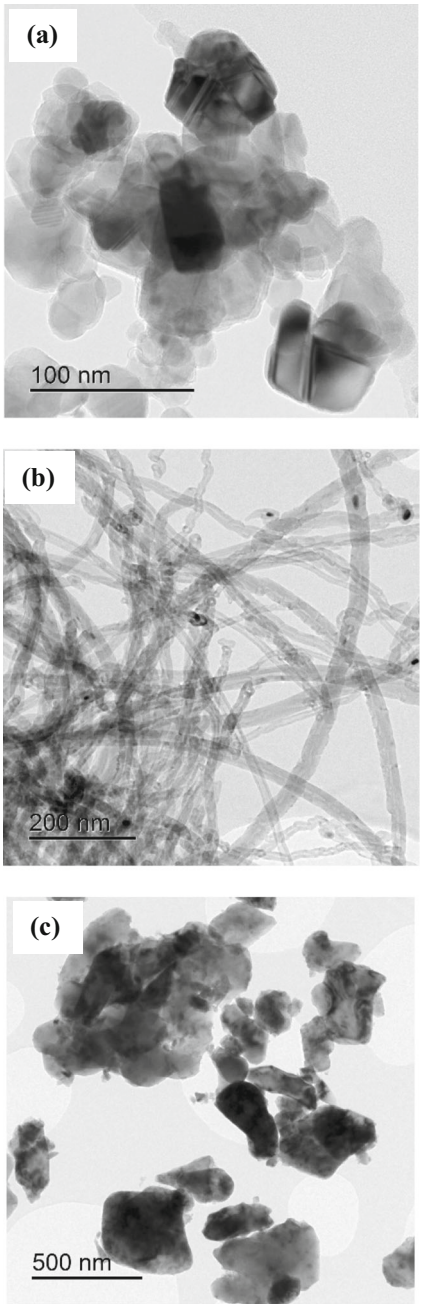

Fig. 1 TEM images of powders (**a**) SiC, (**b**) CNTs, and (**c**) Al_2O_3

distribution, as shown in Fig. 1a, with an average size of approximately 50 nm. The treatment of the carbon nanotubes removed the catalyst, opened the tube caps, and formed holes on the sidewalls. Furthermore, the CNTs were oxidized to generate $COOH^-$ functional groups. The CNTs were less agglomerated, as seen in Fig. 1b, due to the presence of electrostatic repulsive forces, which can overcome Van der Waals attraction forces. Figure 1c shows the alumina nanopowder, which has a particle size distribution with an average size of 200 nm.

Typical FE-SEM images of the Al_2O_3-5SiC-1CNT nanocomposite powder and X-ray mapping of silicon and carbon are presented in Fig. 2. The powder appears to have a wide particle size distribution, as shown in Fig. 1a, b. From Fig. 2e, f, it can be inferred that the SiC and CNTs are uniformly dispersed in the nanocomposite powder. Furthermore, Fig. 2c shows that CNTs are uniformly embedded in the alumina matrix as indicated by white arrows. Figure 3a shows an FE-SEM image of the spark plasma sintered Al_2O_3 reference material. From the image, it appears that the alumina matrix did not experience significant grain growth. The monolithic alumina sample demonstrated an intergranular fracture mode. Typical FE-SEM images of the Al_2O_3-5SiC-1CNT sintered composite are presented in Fig. 3b, c, and X-ray mapping of silicon and carbon are shown in Fig. 3e, f, respectively. It can be concluded that the uniform dispersion of SiC particles and CNTs obtained by molecular level mixing and sonication was maintained in the sintered sample. The Al_2O_3-5SiC-1CNTs composite demonstrated a complete transgranular fracture mode compared with the intergranular mode in the alumina sample. In addition, the SiC and CNTs restricted the growth of alumina matrix grains, as shown in Fig. 3b, when compared with the monolithic alumina, shown in Fig. 3a. This is due to grain boundary pinning by the reinforcements [5, 22, 23].

Notably, grain growth occurs during sintering because of the dependence of grain size on temperature and time, which is generally described for isothermal treatments by the following simple equation:

$$G^n - G_0^n = Kt \tag{1}$$

where G_0 and G are the grain sizes at an initial time t_0 and a dwell time t, respectively. K is a temperature-dependent material constant usually expressed with the following Arrhenius equation:

$$K = K_0 \exp\left(\frac{-Q}{RT}\right) \tag{2}$$

where Q is the activation energy for grain growth, R is the gas constant, and T is temperature.

However, the use of molecular level mixing and spark plasma sintering methods enables the development of a hybrid nanocomposite with a uniform distribution of reinforcing agents but also with a small grain size in the matrix.

Densification

Figure 4 shows the relative density values of the sintered samples. Clearly, the sintering temperature had a significant influence on the densification of the composite materials. The

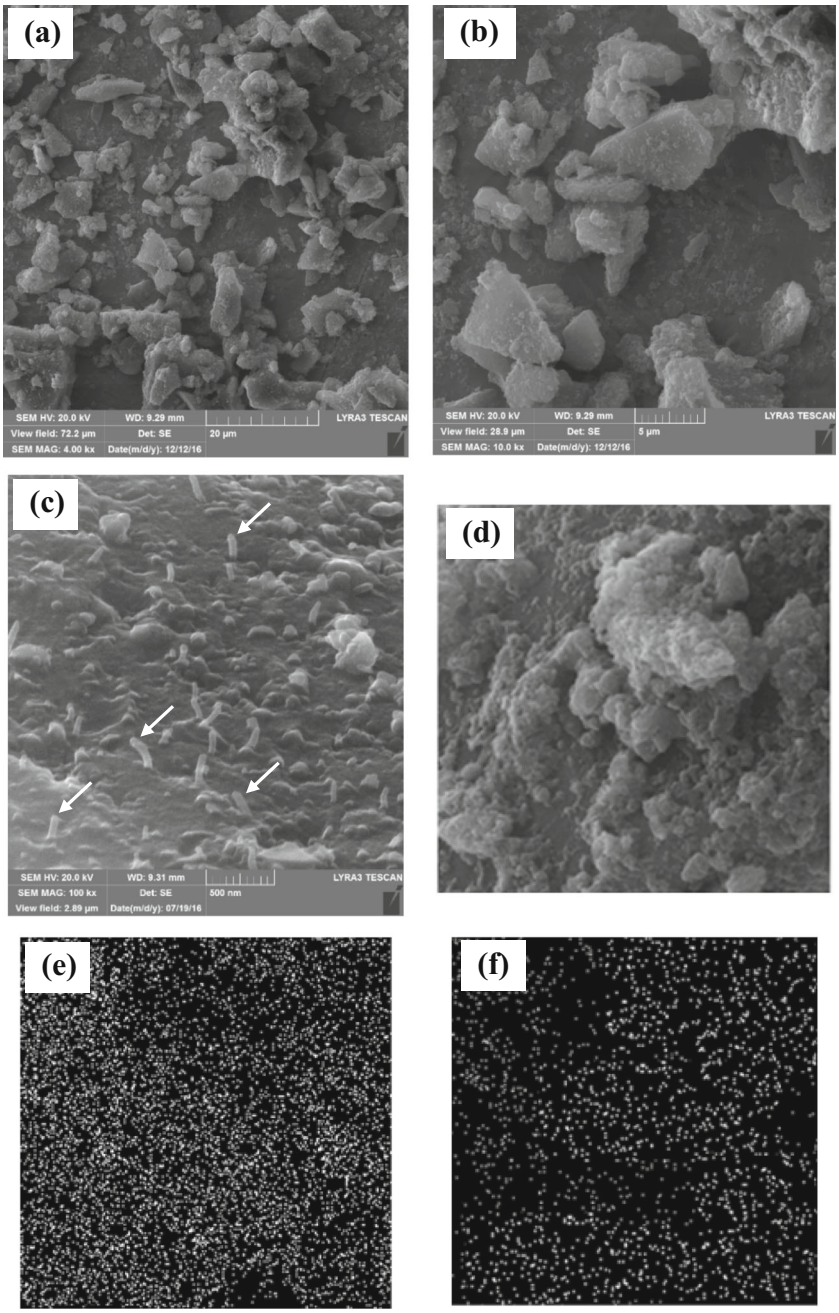

Fig. 2 Typical FE-SEM images of the synthesized Al_2O_3-5SiC-1CNT powder at magnifications of **a** 4000, **b** 10,000, and **c** 100,000. **d** FE-SEM image of the powder and its corresponding x-ray mapping of **e** silicon and **f** carbon

sample which was sintered at 1500 °C had a relative density of 90.36%. Increasing the sintering temperature to 1550 °C increased the relative density to 95.16%. A further increase in the sintering temperature to 1600 °C increased the relative density to 98.9%. The relative density value (90.36%) of the sample sintered at 1500 °C is comparable to the value achieved for the same sample prepared by molecular level mixing using a sonication time of 24 h and spark plasma sintering at 1500 °C for 10 min under an applied pressure of 50 MPa (91.65%) [4]. The high relative density (98.9%) of the hybrid composite sintered at 1600 °C is very similar to the relative density of monolithic alumina (99.3%) sintered at 1500 °C for 10 min [4] and is higher than the values reported for Al_2O_3-SiC-CNT (95.1%) [20] and Al_2O_3-CNT-SiC hybrid nanocomposites (96.4%) [21] spark plasma sintered at 1550 °C and 50 MPa. However, it is comparable with the values reported for alumina hybrid nanocomposites [5, 22–24], including Al_2O_3-SiC-CNTs (greater than 98%) obtained by spark plasma sintering at 1500 °C for 10 min under an applied pressure of 50 MPa [5], Al_2O_3-graphene-CNT (at least 98%) prepared by SPS at 1650 °C for 10 min and 40 MPa [24], Al_2O_3–GNPs-CNTs composites (at least 97.35%) obtained by SPS at 1500 °C for 3 min and 50 MPa [22], and Alumina-TiC-Ni (as high as 98%) [23].

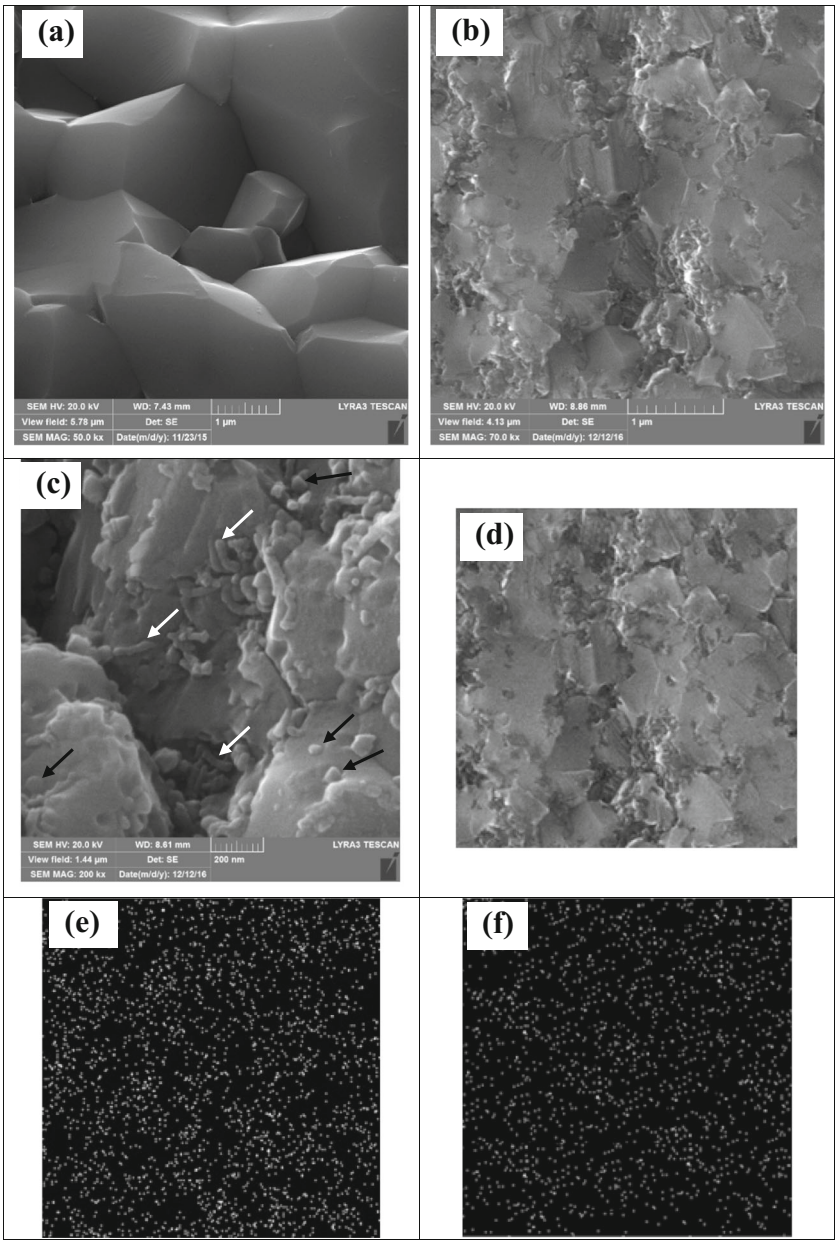

Fig. 3 Typical FE-SEM images of spark plasma sintered (**a**) reference monolithic alumina sample, Al_2O_3-5SiC-1CNT composite at magnifications of (**b**) 70,000 and (**c**) 200,000. (**d**) FE-SEM image of the sintered composite its corresponding x-ray mapping of (**e**) silicon and (**f**) carbon

Although monolithic alumina sinters poorly and the addition of reinforcement to a ceramic matrix is known to reduce the densification [5], the high density reached in this work shows that almost fully dense alumina and Al_2O_3-5SiC-1CNT composites could be processed using spark plasma sintering. For spark plasma sintered materials, the degree of densification depends several variables, particularly the sintering temperature and time, applied pressure, and current. The dependence of the relative density on sintering temperature may be expressed as [25]:

$$\rho = s\left(\frac{T}{T_m}\right) + b \tag{3}$$

where ρ is the relative density, s is the temperature sensitivity, T is the sintering temperature, and T_m is the melting temperature. In the SPS process, it is believed that the spark discharge generates a local high temperature state on the surface of particles. Accordingly, the subsequent evaporation, melting, and formation of necks that occur at the contact point between particles significantly increases the diffusion rate and leads to high final densities. In addition to the Joule heating and the electrical field diffusion effect, the formation of a spark plasma improves overall sintering.

Furthermore, the rearrangement of particles and the breakdown of agglomerates due to externally applied pressure contribute to an increase in the driving force for sintering. In pressure-assisted sintering processes, such as SPS, the

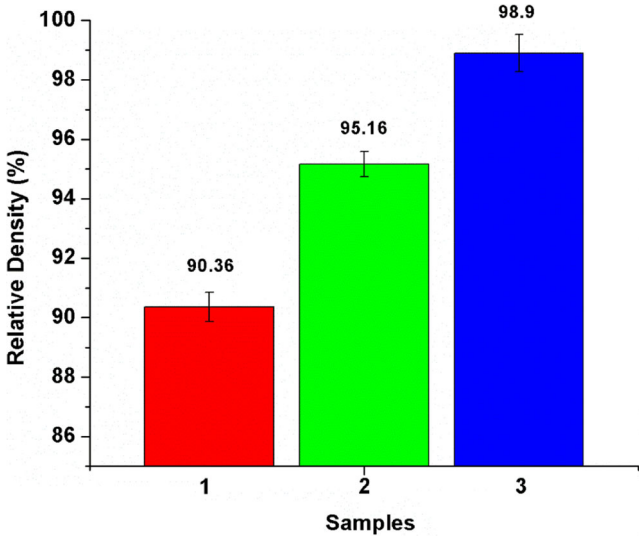

Fig. 4 Relative density of samples sintered at (1) 1500 °C, (2) 1550 °C, and (3) 1600 °C

pressure plays a significant role, and specifically has a large effect on nanopowders. The driving force for sintering depends on the pressure as follows [26]:

$$\frac{d\rho}{(1-\rho)dt} = B\left(g\frac{\gamma}{x} + P\right) \tag{4}$$

where ρ is the relative density, B is a term that includes the diffusion coefficient and temperature, g is a geometric constant, γ is the surface energy, x is a parameter that represents a size scale (and hence is related to particle size), t is time, and P is the applied external pressure.

Additionally, nanoparticles exhibit a high tendency to undergo sintering, largely due to the effect of curvature [27]. The resulting increased total equilibrium vacancy concentration in a nanoparticle can be expressed as follows:

$$X_V^{Total} = \exp\left(-\frac{\Delta G_v^{bulk}}{k_B T}\right)\exp\left(-\frac{\Omega\gamma}{rk_B T}\right) \tag{5}$$

where ΔG_v^{bulk} is the equilibrium Gibbs free energy change for the formation of vacancies in the bulk, Ω is the atomic volume, γ the surface energy, r the radius of curvature, K_B is the Boltzmann constant, and T is temperature.

The role of current can be understood through Joule heating, which is related to the root mean squared of the instantaneous current intensity as follows [28]:

$$I_{RMS} = \sqrt{\frac{1}{\tau}\int_t^{t+\tau} I^2 t(dt)} \tag{6}$$

where I represents the current and τ the sampling time.

Although Al_2O_3 is known as an insulator, it was reported that an Al_2O_3-5SiC-1CNT hybrid composite prepared by ball milling and spark plasma sintering at 1500 °C for 10 min had an electrical conductivity of 4.28 S/m, which is significantly higher than the value for monolithic alumina of 6.87×10^{-10} S/m [29]. This change in behavior from an insulating alumina to an electrically conducting composite may enhance the role of the applied current and improve the densification of the composite. An improvement in density by reinforcing alumina with conducting or semi-conducting phases such as Ni, SiCw, and TiC has been reported by other researchers [23, 30, 31].

Equations 3 and 4 indicate that the temperature and pressure play a significant role in the densification process. Additionally, the small size of the nanoparticles coupled with the additional driving force provided by the current for sintering, which can be inferred from eqs. 5 and 6, respectively, further increases the density of the composite. This leads to high relative density values and hence low porosity, as achieved in this work. The degree of densification is an indication of a good dispersion of the reinforcing agents and would normally lead to a greater hardness and toughness.

Hardness

The hardness values of the sintered samples are presented in Fig. 5. The sample sintered at 1500 °C had a hardness of 16.9 GPa. Increasing the sintering temperature to 1550 °C consequently increased hardness to 19.75 GPa. A further increase in the sintering temperature to 1600 °C increased the hardness to 23.32 GPa; this is notably high when compared to the value obtained for a monolithic alumina reference sample sintered at 1500 °C for 10 min (18.56 GPa) [4] and constitutes an increase in hardness of 25.65%. The increase in the hardness corresponding to the increase in temperature is mainly a result of the increase in densification, as was explained above. The hardness of the Al_2O_3-SiC-CNT composite could be attributed to the small grain size of the alumina matrix, as shown in Fig. 3b, as well as the excellent mechanical properties of the reinforcements. SiC is known to have a hardness of approximately 30 GPa, while the hardness of alumina is approximately 17.65 GPa [32]. Furthermore, CNTs are known for their outstanding mechanical properties [33, 34].

The hardness value of 23.32 GPa achieved in this work is higher than the hardness values reported for Al_2O_3-SiC-CNT [4, 5, 20, 21], Al_2O_3-SiC_w-TiC [30, 31], and Al_2O_3-GNT-CNT [24] hybrid nanocomposites, but lower than the hardness values of 24.65 and 25.6 GPa reported for Al_2O_3-SiC-GNPs [22] and Al_2O_3-Ni-TiC [23], respectively.

A hardness of 20.81 GPa was reported for Al_2O_3-10SiC-1CNTs prepared by ball milling and spark plasma sintering, which can be contrasted with the hardness of 18.56 GPa for pure alumina [5]. The improvement in hardness was attributed

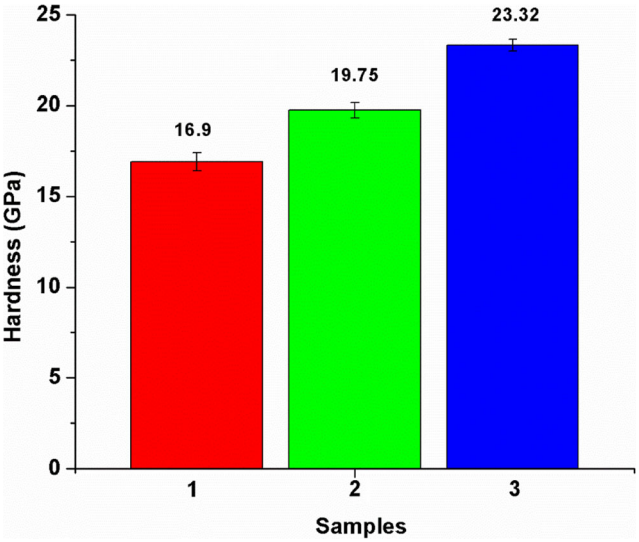

Fig. 5 Hardness of samples sintered at (1) 1500 °C, (2) 1550 °C, and (3) 1600 °C

to the presence of a SiC hard phase and to the small grain size of the alumina matrix in the Al_2O_3-10SiC-1CNTs composite [5]. The addition of 22 vol.% of TiC to Al_2O_3-SiCw [30, 31] reportedly increased the hardness from 15.85 to 22.74 GPa. In another investigation, the addition of 0.38 vol.% of GNPs to Al_2O_3-SiC (1, 3, 5 vol.% SiC) [22] was found to increase the hardness from 18.04 up to 24.65 GPa; however, this composite only demonstrated a 50% increase in fracture toughness. Other researchers have reported that the hardness values of almost fully densified (> 98%) Al_2O_3-GNPs-CNT nanocomposites increased from 13.5 GPa (monolithic alumina) up to 15.5 GPa (Al_2O_3–0.5wt.GNT-1wt.%CNT), but then decreased to 11.2 GPa (Al_2O_3-1wt.GNT-1wt.%CNT) with the addition of more GNTs [24]. In another study [23], a hardness value of 25.6 GPa was reported for an Al_2O_3–1.9 vol.% nNi −25 vol.% nTiC nanocomposite compared to a hardness of 19.9 GPa for pure alumina; however, this composite had a low fracture toughness of 3.7 MPa.m$^{1/2}$. The increase in hardness was attributed to a hardening effect brought about by the Ni and TiC nanoparticles [23]. In other reports [4, 20, 21], Al_2O_3-SiC-CNT hybrid nanocomposites were found to have a lower hardness than monolithic Al_2O_3. A hardness value of 17 GPa was reported for monolithic Al_2O_3, while hardness values between 14 and 17 GPa were reported for the Al_2O_3-5 vol% CNT composite reinforced with 1, 2, or 3 vol% SiC [21] and for the Al_2O_3-1vol%SiC composite reinforced with 5, 7, or 10 vol% CNTs [20]. Additionally, the Al_2O_3-5SiC-1CNT composite synthesized by molecular level mixing using a sonication time of 24 h and spark plasma sintering at 1500 °C for 10 min, was found to have a hardness value of 17.81 GPa compared to a value of 18.56 GPa for monolithic alumina. The low hardness values for the hybrid composites were attributed to low overall densification [4, 20, 21].

In summary, the addition of hybrid reinforcements to alumina has been reported to increase hardness [5, 22–24, 30, 31], with a few exceptions [4, 20, 21] where the hardness was found to decrease. The increase in hardness for alumina hybrid nanocomposites was attributed to the following: (i) the presence of hard reinforcing phases, (ii) the small grain size of the alumina matrix, which is due to the pinning effect of the reinforcements, and (iii) the high level of densification. The decrease in hardness was believed to be due to the reduced densification and the presence of softer phases at the grain boundaries, including CNTs which have low hardness values in the radial direction. Additionally, weak interfaces between the reinforcing agents and Al_2O_3, the lubricating nature of some reinforcements such CNTs and graphene, and the agglomeration of the reinforcing nanoscale phases [35] may offset both the advantages of the SPS process and the influence of microstructure refinement due to pinning effects by the reinforcements [36–38]. Notably, hardness is known to be sensitive to the testing load [39] and to residual internal stresses [40], which result from a thermal mismatch between Al_2O_3 and the reinforcement.

Fracture toughness

Figure 6 shows the fracture toughness values of the sintered samples. The sample sintered at 1500 °C had a fracture toughness of 5.68 MPa.m$^{1/2}$. An increase in sintering temperature to 1550 °C increased the fracture toughness to 6.12 MPa.m$^{1/2}$. A further increase in the sintering temperature up to 1600 °C increased the fracture toughness to 7.10 MPa.m$^{1/2}$; this value is very high compared to the 3.61 MPa.m$^{1/2}$ value for a monolithic alumina reference sample sintered at 1500 °C for 10 min [4]. This constitutes an increase in fracture toughness of 96.67%. The increase in fracture toughness may be attributed to a change in the fracture mode from an intergranular fracture for the monolithic alumina to a complete transgranular fracture mode for the hybrid composite, which is shown in Fig. 3a, b, respectively. Furthermore, toughening mechanisms such as crack deflection, crack bridging, CNT breaking, and CNT pull-out, as shown in Fig. 7, contribute to the overall improvement in fracture toughness. Additionally, the removal of residual stresses through the generation of dislocations around the reinforcement particles is believed to improve fracture toughness [41, 42].

The addition of hybrid nanoreinforcements to alumina has been reported to increase [4, 5, 20–24, 31, 43–45] or decrease [46] its fracture toughness. The fracture toughness value obtained for the sample sintered at 1500 °C (5.68 MPa.m$^{1/2}$) is slightly higher than the value achieved for the same sample prepared by molecular level mixing using a sonication time of 24 h and spark plasma sintered at 1500 °C for 10 min under an applied pressure of 50 MPa (5.38 MPa.m$^{1/2}$) [4]. The high fracture toughness value achieved in this work (7.10 MPa.m$^{1/2}$) is

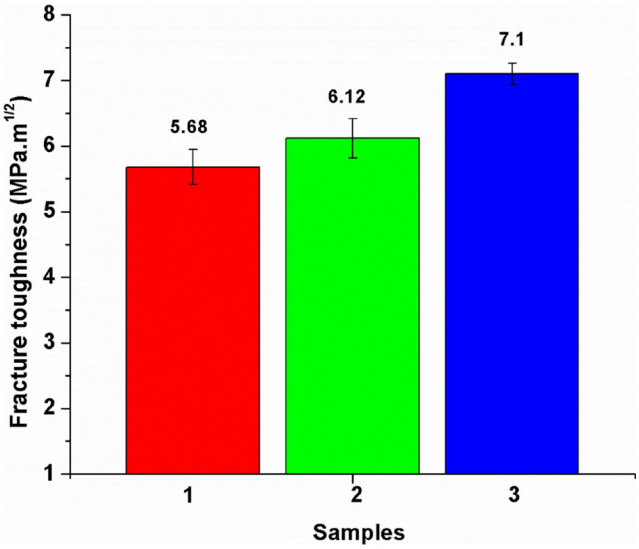

Fig. 6 Fracture toughness of samples sintered at (1) 1500 °C, (2) 1550 °C, and (3) 1600 °C

higher than fracture toughness values reported for spark plasma sintered alumina hybrid nanocomposites [4, 5, 20–24, 31, 43–46]. A fracture toughness value of 6.98 MPa.m$^{1/2}$ was reported for an Al_2O_3-10SiC-2CNT composite, which can be compared to a value of 3.61 MPa.m$^{1/2}$ obtained for alumina [5]. In another study, fracture toughness values up to approximately 6 MPa.m$^{1/2}$ were reported for Al_2O_3-5 vol% CNT composites reinforced with 1, 2, or 3 vol% SiC [21] and for Al_2O_3-1vol%SiC composites reinforced with 5, 7, or 10 vol% CNTs [20]. The improvement in fracture toughness was attributed to the strengthening of grain boundaries and to the toughening of the alumina matrix by SiC nanoparticles combined with fiber toughening mechanisms from the MWCNTs. "The incorporation of SiC nanoparticles is also believed to remove residual stresses at the alumina-alumina boundaries, and in matrix grains by generating dislocations around the particles [41, 42]. Elimination of tensile stresses strengthens the grain boundaries and impedes the intergranular fracture observed in alumina with added CNTs." The addition of 0.38 vol.% of GNPs to Al_2O_3-SiC (1, 3, 5 vol.% SiC) [22] was found to increase the fracture toughness to a maximum of 5.03 MPa.m$^{1/2}$. In another report, the addition of GNPs to Al_2O_3 was reported to increase the fracture toughness and decrease the hardness [43]. However, an Al_2O_3 hybrid nanocomposite reinforced with both GNPs and SiC nanoparticles showed approximately a 36% and a 50% increase in hardness and fracture toughness, respectively [22]. This increase was attributed to the fact that the SiC nanoparticles helped to achieve a good dispersion of GNPs, decreased the average grain size of alumina, and increased the

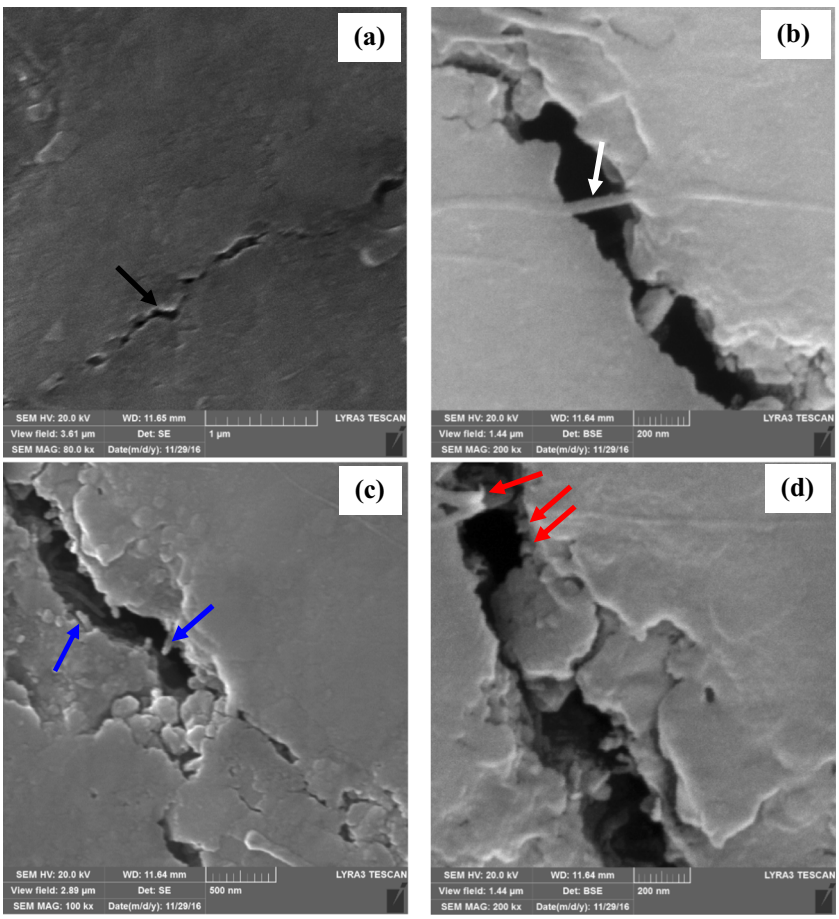

Fig. 7 FE-SEM images of Al_2O_3-5SiC-1CNT nanocomposite, sintered at 1600 °C, revealing toughening mechanisms (a) crack deflection (b) crack bridging, CNT breaking, and (d) CNT pullout

hardness. Furthermore, the presence of the GNPs improved the fracture toughness by crack bridging, GNP pullout, and crack deflection mechanisms. In another study, the fracture toughness of an Al_2O_3-GNPs-CNT nanocomposite was found to increase up to 5.75 MPa.m$^{1/2}$ for a sample containing 0.5 GNPs and 0.5 CNTs [24]. The improvement in fracture toughness was attributed to the role of the GNPs in anchoring around the alumina grains and in increasing the interfacial friction between the reinforcing agents and the alumina matrix. This increases the required energy for GNP pull-out, leading to a transgranular fracture mode. In addition, both GNPs and CNTs can stop cracks from propagating through a bridging mechanism. As with GNPs, CNTs can also strengthen grain boundaries and change the fracture mode to transgranular fracture. The addition of 22 vol.% TiC to an Al_2O_3-SiCw composite [31] was reported to increase the fracture toughness to 6.5 MPa.m$^{1/2}$. This increase was attributed to the presence of TiC particles, which are known to significantly improve the fracture toughness of alumina [44, 45]. However, in another investigation, only a marginal improvement in the fracture toughness was reported, from 3.5 MPa.m$^{1/2}$ (Al_2O_3) up to 3.7 MPa.m$^{1/2}$ (Al_2O_3–1.9 vol.% nNi −25 vol.% nTiC) [23]. The use of carbon fibers and SiC [46] was reported to decrease the fracture toughness of a Al_2O_3-20vol.%CNF-10vol.SiC composite to as low as 2.79 MPa.m$^{1/2}$.

In conclusion, the fracture toughness of an alumina hybrid nanocomposite depends on the following factors: (i) the nature, amount and degree of dispersion of the reinforcements, (ii) the level of densification, (iii) the quality and strength of the interface, and (iv) the toughening mechanisms induced by the nanoreinforcements.

Conclusions

Fully dense, hard, and tough Al_2O_3-SiC-CNT hybrid nanocomposites were successfully produced via molecular level mixing and spark plasma sintering methods. The influence of sintering temperature on the microstructure, densification, hardness, and fracture toughness of the composite was investigated. The synthesized nanopowder and the consolidated samples demonstrated a uniform distribution of the SiC and CNT reinforcements. The relative density of sintered samples increased from 90.36 to 98.91% with a corresponding increase in sintering temperature from 1500 to 1600 °C. The Al_2O_3-5SiC-1CNT composite sintered at 1600 °C for 10 min possessed the highest hardness and fracture toughness values of 23.32 GPa and 7.10 MPa.m$^{1/2}$, respectively. This constitutes an increase in hardness and fracture toughness of 25.65 and 96.67%, respectively, compared to monolithic alumina sintered at 1500 °C for 10 min. The concurrent increase in hardness and fracture toughness is attributed to the uniform distribution of the reinforcements, to high densification, to the refinement of the alumina matrix grain size, to a change in fracture mode and to the toughening mechanisms brought about by the SiC nanoparticles and the CNTs.

Acknowledgments The authors would like to acknowledge the King Abdulaziz City for Science and Technology (KACST) for funding this work through project AR-34-3.

Compliance with ethical standards

Conflict of interest The authors declare that they have no conflict of interest.

References

1. Carter C.B., Norton M.G.: Ceramic Materials, Science and Engineering, 2nd Ed. Springer, (2013)
2. Low, I.M: Advances in ceramic matrix composites: an introduction. In: Low, I.M., (ed.) Adv. Ceram. Matrix Compos. Elsevier. p. 1 (2014)
3. Palmero, P.: Structural, ceramic nanocomposites: a review of properties and powders' synthesis methods. Nanomaterials. **5**, 656 (2015)
4. Mohammad, K., Saheb, N.: Molecular level mixing: an approach for synthesis of homogenous hybrid ceramic nanocomposite powders. Powder Technol. 291, 121 (2016)
5. Saheb, N., Mohammad, K.: Microstructure and mechanical properties of spark plasma sintered Al2O3-SiC-CNTs hybrid nanocomposites. Ceram. Int. 42, 12330 (2016)
6. Ahmad, I., Islam, M., Subhani, T., Zhu, Y.: Toughness enhancement in graphene nanoplatelet/SiC reinforced Al_2O_3 ceramic hybrid nanocomposites. Nanotechnology. 27, 425704 (2016)
7. Ahmad, I., Ahmed, S., Subhani, T., Saeed, K., Islam, M., Wang, N.: Synergic influence of MWCNTs and SiC nanoparticles on the microstructure and properties of Al_2O_3 ceramic hybrid nanocomposites. Curr. Appl. Phys. 16, 1649 (2016)
8. Cha, S.I., Kim, K.T., Arshad, S.N., Mo, C.B., Hong, S.H.: Extraordinary Strengthening Effect of Carbon Nanotubes in Metal-Matrix Nanocomposites Processed by Molecular-Level Mixing. Adv. Mater. 17(11), 1377 (2005)
9. Lee, B., Koo, M.Y., Jin, S.H., Kim, K.T., Hong, S.H.: Simultaneous strengthening and toughening of reduced graphene oxide/alumina composites fabricated by molecular-level mixing process. Carbon. 78, 212 (2014)
10. Cha, S.I., Kim, K.T., Lee, K.H., Mo, C.B., Hong, S.H.: Strengthening and toughening of carbon nanotube reinforced alumina nanocomposite fabricated by molecular level mixing process. Scr. Mater. 53, 793 (2005)
11. Saheb N., Iqbal Z., Khalil A., Hakeem A.S., Al-Aqeeli N., Laoui T., Al-Qutub A., Kirchner R.: Spark plasma sintering of metals and metal matrix nanocomposites: a review. J. Nanomater. Article ID 983470, p.1, (2012)
12. Suárez M., Fernández A., Menéndez J.L., Torrecillas R., Kessel H. U., Hennicke J., Kirchner R., Kessel T.: Challenges and Opportunities for Spark Plasma Sintering: A Key Technology for a New Generation of Materials, chapter 13, In Sintering Applications, Book Edited by Burcu Ertuğ, Published by InTech, p. 319 (2013)
13. Zhang, Z.-H., Liu, Z.-F., Lu, J.-F., Shen, X.-B., Wang, F.-C., Wang, Y.-D.: The sintering mechanism in spark plasma sintering – Proof of the occurrence of spark discharge. Scr. Mater. 81(15), 56 (2014)

14. Munro, R.G.: Evaluated Material Properties for a Sintered α-Alumina. J. Am. Ceram. Soc. 80 (8), (1997, 1919)
15. Liu, B.Q., Huang, C.Z., Sun, A.L.: Toughening mechanisms and wear behavior of a TiC whisker toughening alumina ceramic cutting tool composite. Adv. Mater. Res. 500, 634 (2012)
16. Mozalev, A., Sakairi, M., Takahashi, H., Habazaki, H., Hubálek, J.: Nanostructured anodic-alumina-based dielectrics for high-frequency integral capacitors. J. Thin Solid Films. 550, 486 (2014)
17. Martin CA, Lee GF, Fedderly JJ.: US Patent 8, 387, 510 (2013)
18. Andrievski, R.A.: Synthesis, structure and properties nanosized silicon carbide. Rev. Adv. Mater. Sci. 22, 1 (2009)
19. Iijima, S.: Helical microtubules of graphitic carbon. Nature. 354, 56 (1991)
20. Ahmad, K., Pan, W.: Hybrid nanocomposites: a new route towards tougher alumina ceramics. Compos. Sci. Technol. 68, 1321 (2008)
21. Ahmad, K., Pan, W., Qu, Z.: Multifunctional properties of alumina composites reinforced by a hybrid filler. Int. J. Appl. Ceram. Technol. 6, 80 (2009)
22. Liu, J., Li, Z., Yan, H., Jiang, K.: Spark plasma sintering of alumina composites with graphene platelets and silicon carbide nanoparticles. Adv. Eng. Mater. 16, 1111 (2014)
23. Rodriguez-Suarez, T., Bartolomé, J.F., Smirnov, A., Lopez-Esteban, S., Díaza, L.A., Torrecillas, R., Moya, J.S.: Electroconductive Alumina-TiC-Ni nanocomposites obtained by Spark Plasma Sintering. Ceram. Int. 37 (5), 1631 (2011)
24. Yazdani, B., Porwal, H., Xia, Y., Yan, H., Reece, M.J., Zhu, Y.: Role of synthesis method on microstructure and mechanical properties of graphene/carbon nanotube toughened Al_2O_3 nanocomposites. Ceram. Int. 41, 9813 (2015)
25. Garay, J.E.: Current-activated, pressure-assisted densification of materials. Annu. Rev. Mater. Res. 40, 445 (2010)
26. Munir, Z.A., Tamburini, U.A., Ohyanagi, M.: The effect of electric field and pressure on the synthesis and consolidation of materials: a review of the spark plasma sintering method. J. Mater. Sci. 41, 763 (2006)
27. Ashby M.F., Ferreira P.J., Schodek D.L.: Nanomaterials, Nanotechnologies and Design: An Introduction for Engineers and Architects, Elsevier Ltd. 2009
28. Orrù, R., Licheri, R., Locci, A.M., Cincotti, A., Cao, G.: Consolidation/synthesis of materials by electric current activated/assisted sintering. Mater. Sci. Eng. R. 63, 127 (2009)
29. Saheb, N., Hayat, U.: Electrical conductivity and thermal properties of spark plasma sintered Al_2O_3-SiC-CNT hybrid nanocomposites. Ceram. Int. (2017). https://doi.org/10.1016/j.ceramint.2017.01.112
30. Gutiérrez-González, C.F., Suarez, M., Pozhidaev, S., Rivera, S., Peretyagin, P., Solís, W., Díaz, L.A., Fernandez, A., Torrecillas, R.: Effect of TiC addition on the mechanical behaviour of Al_2O_3–SiC whiskers composites obtained by SPS. J. Eur. Ceram. Soc. 36, 2149 (2016)
31. Pozhidaev, S.S., Seleznev, A.E., Solis Pinargote, N.W., Peretyagin, P.Y.: Spark plasma sintering of electro conductive nanocomposite Al2O3-SiCw-TiC. Mech. Ind. 16 (7), 1 (2015)
32. Mohanty, P., Mohapatra, S., Mohapatra, J., Singh, S.K., Padhi, P., Mishra, D.K.: Utilization of chemically synthesized fine powders of SiC/Al2O3 composites for sintering. Mater. Manuf. Process. 29, 1–7 (2016)
33. Yu, M.F., Lourie, O., Dyer, M.J., Moloni, K., Kelly, T.F., Ruoff, R.S.: Strength and breaking mechanism of multiwalled carbon nanotubes under tensile load. Science. 287, 640 (2000)
34. Hayashi, T., Endo, M.: Carbon nanotubes as structural material and their application in composites. Compos B. 42, 2151 (2011)
35. Galusek, D., Galusková, D.: Alumina matrix composites with non-oxide nanoparticle addition and enhanced functionalities. Nanomaterials. 5, 115 (2015)
36. Ahmad, I., Unwin, M., Cao, H., Chen, H., Zhao, H., Kennedy, A., Zhu, Y.Q.: Multi-walled carbon nanotubes reinforced Al_2O_3 nanocomposites: mechanical properties and interfacial investigations. Comp. Sci. Technol. 70, 1199 (2010)
37. Vasiliev, A.L., Poyato, R., Padture, N.P.: Single-wall carbon nanotubes at ceramic grain boundaries. Scr. Mater. 56, 461 (2007)
38. Gao, L., Jiang, L., Sun, J.: Carbon nanotube-ceramic composites. J Electroceram. 17, 51 (2006)
39. J. Wade, and H. Wu, Hardness of alumina/silicon carbide nanocomposites at various silicon carbide volume percentages. Mathur, S. et al. (eds) Ceramic Engineering and Science Proceedings. Nanostructured Materials and Nanotechnology VII. Hoboken: Wiley. 34(2013) 7, 119
40. Wana, Y., Gong, J.H.: Influence of TiC particle size on the load-independent hardness of Al_2O_3–TiC composites. Mater. Lett. 57, 3439–3443 (2003)
41. Xia, Z., Riester, L., Curtin, W.A., Li, H., Sheldon, B.W., Liang, J., Chang, B., Xu, J.M.: Direct observation of toughening mechanisms in carbon nanotube ceramic matrix composites. Acta. Mater. 52, 931 (2004)
42. Xia, Z., Curtin, W.A., Sheldon, B.W.: Fracture toughness of highly ordered carbon nanotube/alumina nanocomposites. J. Eng. Mater. Technol. Trans. ASME. 126, 238 (2004)
43. Liu, J., Yan, H., Jiang, K.: Mechanical properties of graphene platelet-reinforced alumina ceramic composites. Ceram. Int. 39 (6), 6215 (2013)
44. Gong, J., Zhao, Z., Miao, H., Guan, Z.: R-curve behavior of TiC particle reinforced Al_2O_3 composites. Scr. Mater. 43, 27 (2000)
45. Gong, J., Zhao, Z., Guan, Z.: On the local crack resistance of Al_2O_3–TiC composites evaluated by direct indentation method. J. Eur. Ceram. Soc. 21, 941 (2001)
46. Umino, K., Wakayama, S., Sakai, T., Umehara, Y., Akatsu, T.: Mechanical Properties of CNF Reinforced Ceramic Composites Sintered with SPS Technique. J. Solid Mech. Mater. Eng. 5(12), 866 (2011)